3D UWB Magnitude-Combined Tomographic Imaging for Biomedical Applications. Algorithm Validation

Marta GUARDIOLA, Lluís JOFRE, Santiago CAPDEVILA, Sebastián BLANCH, Jordi ROMEU

AntennaLab, Universitat Politècnica de Catalunya, C/ Jordi Girona 3-4, 08034 Barcelona, Spain

marta.guardiola@tsc.upc.edu, jofre@tsc.upc.edu, scapdevila@tsc.upc.edu, blanch@tsc.upc.edu, romeu@tsc.upc.edu

Abstract. *Biomedical microwave imaging is a topic of continuous research for its potential in different areas especially in breast cancer detection. In this paper, 3D UWB Magnitude-Combined tomographic algorithm is assessed for this recurrent application, but also for a more challenging one such as brain stroke detection. With the UWB Magnitude-Combined concept, the algorithm can take advantage of both the efficiency of Fourier Diffraction Theorem-based tomographic formulation and the robustness and image quality improvement provided by a multi-frequency combination.*

Keywords

Tomography, biomedical imaging, microwave imaging, breast cancer, brain stroke, experimental verification.

1. Introduction

Microwave imaging is a topic of intense research for its potential in biomedical applications and especially in breast cancer detection. X-ray mammography is the generally well-established clinical breast imaging technique for preventive screening and cancer treatment. Other imaging techniques including MRI (magnetic resonance imaging), ultrasounds or PET (positron emission tomography), are recommended for cases where X-ray mammography does not succeed, such as in women with dense breasts or with high cancer risk to avoid exposition to ionizing radiation, as reported in [1]. This, jointly with other concerns, such as the ionizing character of X-ray radiation, its uncomfortable (and even painful) application, motivate the research in complementary or alternative imaging methods exploiting other physical properties of tissues. In this framework, the potential of microwave imaging relies on the capability of microwaves to differentiate among tissues based on the contrast in dielectric properties, which is more important than those exploited by X-ray mammography (the attenuation of waves when passing through the breast structures) [2]. The advantages for its practical clinical usage are significant, including relatively low cost, the use of low-power non-ionizing radiation and patient comfort.

Active microwave imaging relies on obtaining information about a target from the scattered fields measured at a number of probes, when the target is illuminated with an incident field. This inverse scattering problem can be addressed either by radar-based techniques (refer to [3] for a review of UWB radar methods) or tomographic methods. Tomographic approaches try to solve the non-linear and ill-posed inverse scattering problem, by either linearizing it or iteratively approaching the solution. Many research groups are focused on iterative algorithms to obtain quantitative reconstructions of the dielectric properties of the target. Those are computationally intensive, above all for 3D reconstructions, and usually contain some regularization scheme that requires *a priori* information about the target, having a direct influence into the algorithm convergence [4]. A number of different methods and optimization schemes have been proposed, [5]-[7], reporting useful 3D reconstructions of numerical models, phantoms and first 2D measurements on real patients [8]. However more research towards increasing computational efficiently of the algorithms is needed for a real time imaging. This opens the door to less computationally heavy algorithms as the ones based on linearizing approximations.

Linearizing approximations, on which the method proposed here is partially based, allow to obtain robust reconstructions, in a very efficient way, being however limited to small relatively low-contrast targets to produce quantitative reconstructions [9]. In general, biological organs do not accomplish these requirements, thus, linearizing methods are restricted to qualitative reconstructions. In [10], useful qualitative images of a transversal cut of a human forearm were presented, retrieving clearly the two bones.

The use of multi-frequency information in a convenient manner has been recognized as an opportunity for linearizing methods to improve the image quality in non-Born scenarios [11]. To this extent, it has not been used in linearized tomography methods due to the well-known frequency-dependent residual phase errors that appear when electrically large and highly contrasted targets are imaged. In the algorithm validated herein, namely 3D UWB Magnitude-Combined (UWB-MC) tomography, an amplitude (phase-less) multi-frequency combination is proposed to overcome this undesired effect [12].

Brain stroke detection is also addressed in this paper to investigate the potentiality of the proposed algorithm in such a challenging application, as proposed previously by [5], [13]. The motivation to explore this case is the difficulty to differentiate the cause of the stroke between a hemorrhage or a blood clot. Both present similar symptoms, but opposite treatment, which must be given with the maximum promptness. Up to now, the diagnosis relies on bulky imaging methods, such as CT (computed tomography), PET and MRI, which are not available in all medical emergency units. This deficiency may definitely delay or complicate the decision and eventually cause important after-effects.

2. 3D UWB Magnitude-Combined Tomographic Imaging Algorithm

3D UWB Magnitude-Combined tomographic imaging, as the name suggests, proposes a compound coherent multi-view image addition, which is typical of the linearized-tomography-based algorithms, followed with a magnitude multi-frequency image combination, in the last step of the algorithm. In this paper a 3D cylindrical geometry, as shown in Fig. 1 is studied. The cylindrical array of both the transmitting and the receiving antennas is composed by N_z, $2a$-diameter rings of N_ϕ angularly equispaced antennas. For a given transmitter, situated at $\vec{r}'_T$, the scattered field is measured at the receiver positions, $\vec{r}'_R$. This procedure is successively repeated for each transmitter to complete a maximum of $N_\phi \times N_z$ acquisitions.

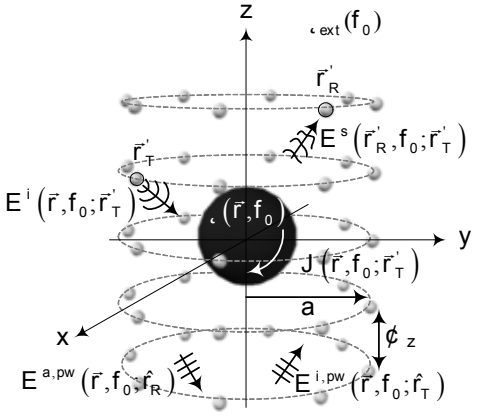

Fig. 1. The target of permittivity $\epsilon(\vec{r}, f_0)$ is immersed in a medium of permittivity $\epsilon_{ext}(f_0)$. The measurement cylindrical array of antennas is composed by N_z rings of N_ϕ antennas of radius a, separated a distance Δ_z. $\vec{r}'_{T,R}$ refers to the position of the transmitting and receiving antennas respectively, and $\hat{r}_{T,R}$ is the direction of the synthesized plane wave.

The theoretical basis for 3D UWB-MC to obtain the dielectric contrast of the target is as follows. Let $c(\vec{r}, f_0)$ be the dielectric contrast expressed as

$$c(\vec{r}, f_0) = 1 - \frac{\epsilon(\vec{r}, f_0)}{\epsilon_{ext}(f_0)} \tag{1}$$

$\epsilon(\vec{r}, f_0)$ and $\epsilon_{ext}(f_0)$ being the complex permittivities of the target and the external medium respectively, measured at a particular frequency f_0.

The dielectric contrast can be related to the induced current on the target, $\vec{J}(\vec{r}, f_0, \vec{r}'_R)$, by

$$\vec{J}(\vec{r}, f_0, \vec{r}'_R) = -j2\pi f_0 \big(\epsilon(\vec{r}, f_0) - \epsilon_{ext}(f_0)\big)\vec{E}^t(\vec{r}, f_0, \vec{r}'_R) = \\ = j2\pi f_0 \epsilon_{ext}(f_0) c(\vec{r}, f_0)\vec{E}^t(\vec{r}, f_0, \vec{r}'_R) \tag{2}$$

where $\vec{E}^t$ is the total electric field including the scattered and the incident field.

Using the reciprocity theorem (3), one can obtain the induced current on the target, $\vec{J}_R$, from the scattered field measured along the antenna

$$\iiint \vec{J}_T \cdot \vec{E}_R \, dv_T = \iiint \vec{J}_R \cdot \vec{E}_T \, dv_R \, . \tag{3}$$

$\vec{J}_T$ is the electric current on the cylindrical antenna acting as a transmitter which radiates a plane wave electric field, $\vec{E}_T$, propagating to a direction $\hat{r}_T$. $\vec{J}_R$ is the electric current on the target induced by a plane wave incident field propagating along the vector $\hat{r}_R$ ($\vec{E}^i_R$). $\vec{E}_R$, is the scattered field produced by $\vec{J}_R$.

When the cylindrical array is composed by linear z-polarized antennas, $\vec{J}_T$ is also z-directed, therefore, only the z component of the $\vec{E}_R$ field is needed, thus permitting a scalar formulation.

Under Born approximation (the scattered field is negligible in front of the incident field), the induced current $\vec{J}_R$ can be expressed as

$$\vec{J}_R(\vec{r}, f_0, \vec{r}'_R) \cong j2\pi f_0 \epsilon_{ext}(f_0) c(\vec{r}, f_0) E^i_R(\vec{r}, f_0, \vec{r}'_R)\, \hat{\theta}_R = \\ = J_R(\vec{r}, f_0, \vec{r}'_R)\, \hat{\theta}_R . \tag{4}$$

Then, replacing (4) in (3), a Fourier transform appears, and the spectrum of the contrast profile can be expressed as

$$\tilde{C}\left(k_{0,ext}(\hat{r}_T + \hat{r}_R)\right) = \frac{a^2}{2\pi f_0 \epsilon_{ext}(f_0)} \sum_{i,j,k,m=1}^{N_\phi, N_z, N_\phi, N_z} E^s_z\left(\vec{r}'_{R_{ij}}, f_0; \vec{r}'_{T_{km}}\right) \\ I_\theta\left(\vec{r}'_{T_{km}}, f_0; \hat{r}_T\right) I_\theta\left(\vec{r}'_{R_{ij}}, f_0; \hat{r}_R\right) \tag{5}$$

where $E^s_z\left(\vec{r}'_{R_{ij}}, f_0; \vec{r}'_{T_{km}}\right)$ is the scattered field measured at a probe positioned at $\vec{r}'_{R_{ij}}$ when an antenna placed at $\vec{r}'_{T_{km}}$ is transmitting. $I_\theta\left(\vec{r}'_{T,R}, f_0; \hat{r}_{T,R}\right)$ represents the amplitude to be applied to a probe situated at $\vec{r}'_{T,R}$ to synthesize a plane wave towards $\hat{r}_{T,R}$ and vertical polarization [15] as a combination of cylindrical waves emanating from a number of probes.

From (5) it can be derived that for a given frequency, when the object is illuminated with an incident plane wave directed to $\hat{r}_T$, the Fourier transform of the scattered field obtained at a direction $\hat{r}_R$ may be translated into the angular spectrum of the dielectric contrast of the target sampled on

the surface of a sphere of radius $k_{0,ext} = 2\pi f_0\sqrt{\mu_{ext}\epsilon_{ext}}$ centered at $-k_{0,ext}\hat{r}_T$, where $\hat{r}_{T,R} = \cos\theta_{T,R}\sin\phi_{T,R}\,\hat{x} + \sin\theta_{T,R}\sin\phi_{T,RT}\,\hat{y} + \cos\theta_{T,R}\,\hat{z}$. Thus, the successive angular scans will fill the spectral domain knowledge as depicted in Fig. 2 [14]. In a similar way, by changing the frequency of the incident wave, the radius of the sphere changes providing more information in the spectral domain.

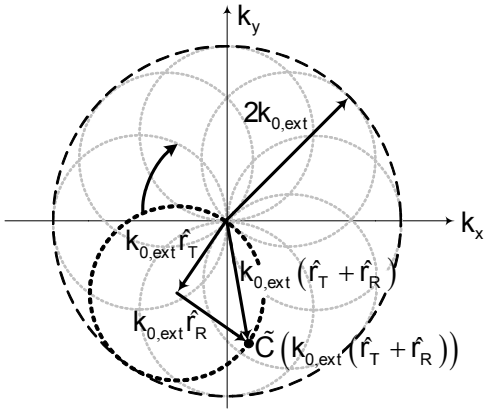

Fig. 2. 2D cut of the dielectric spectrum of the contrast. For a single transmitter and incidence frequency, the spectrum of the contrast is sampled on the surface of a sphere of radius $k_{0,ext}$ centered at $-k_{0,ext}\hat{r}_T$. For another direction of incidence the sphere rotates.

The multi-frequency combination is then obtained by combining only the magnitude of the multi-view images.

$$\tilde{C}_{UWB-MC} = \sum_{i=f_{\min}}^{f_{\max}} \left| FT^{-1}\left(\tilde{C}_{k_{i,ext}}\right)\right| \tag{6}$$

Due to the limited extent of the measurement surface in the z direction, there is a truncation error, which is translated as a deterioration of the synthesized plane wave for $\theta_{T,R}$ close to the nadir or the zenith. Unacceptable plane waves may produce the degradation of the reconstruction and should be avoided. In order to prevent it $\theta_{T,R}$ has been limited between 45º and 135º.

3. Simulation Results

This section gathers the preliminary assessment of UWB-MC tomographic algorithm to study its applicability to biomedical imaging. To do this, breast cancer detection, and a more challenging application, such as brain stroke detection have been considered.

The main goal in biomedical imaging is to develop an imaging method with the best sensitivity, specificity and good spatial resolution. Using microwaves, the requirement of a good spatial resolution can be achieved by using high frequencies; however the attenuation and the number of antennas may become excessive, leading to an unfeasible system. Accordingly, the frequency has to be bounded to a certain value. In this case the synthetic data have been obtained using a full wave simulation software (FEKO) based on the method of moments, over a frequency range between 0.2 - 2 GHz. The number and distribution of the elements in the cylindrical array has been chosen to satisfy the Nyquist spatial sampling criteria in order to avoid aliasing, resulting in $N_z = 12$ rings of $2a = 150$ mm in diameter, composed by $N_\phi = 32$ antennas each one separated $\Delta_z = 1$ cm in the vertical direction.

The breast model consists of a hemispherical body of 90 mm in diameter covered by a 3 mm skin layer attached to the chest wall with a spherical tumor of 8 mm inserted. The breast tissue is modeled as a uniform low-adipose breast tissue; see Fig. 3(a). An external medium of $\epsilon_{ext} = 34$ is used to match the permittivities and ensure the maximum power transmission inside the breast. The frequency dispersive complex permittivity values of the tissues are plotted in Fig. 3(b). In Fig. 4(a) and 4(b) the results of 3D UWB-MC are presented. Fig. 4(a) shows the 3D reconstruction and Fig. 4(b) corresponds to a horizontal cut containing the maximum contrast value, which matches with the center of the tumor. Both figures plot the normalized contrast in permittivities in dB scale. As it can be seen, the images clearly indicate the detected tumor placed at the correct position.

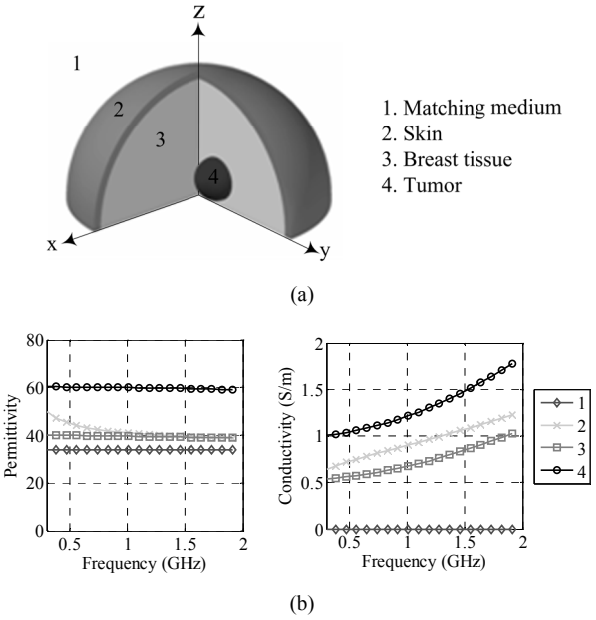

Fig. 3. (a) Simplified breast model composed by a thin skin layer and a uniform low-adipose breast tissue attached to the chest wall with a spherical tumor. (b) Permittivity and conductivity values of the model.

In case of brain stroke detection, the main issue consists of differentiating hemorrhagic from non-hemorrhagic strokes. This can be addressed taking advantage of the sensitivity of microwave radiation to the presence of blood thanks to its high permittivity. In this paper, a simplified brain model is considered as a first approach to the problem. It consists of a semispherical body (equivalent to the upper part of the head) of 180 mm in diameter composed by several layers corresponding to the skin (3 mm of thickness), the skull (2 mm of thickness)

and the brain itself. The brain includes the two hemispheres of white matter covered by a layer of gray matter (20 mm of thickness). The hemorrhage is simulated as a sphere of blood inserted inside the white matter. The geometrical and dielectric properties of the brain model over the frequency are plotted in Fig. 5(a) and 5(b). Due to the significant contrast between the successive layers, and above all due to the important losses of the high-water-content brain tissues, at the current state of development, UWB-MC algorithm is not able to retrieve the stroke without using any assumption about the target. Nevertheless, if functional brain monitoring is considered, sequential differential imaging may be a solution to obtain reliable images of the evolution of intracerebral blood hemorrhages. The subtraction of successive measurements provides a low-contrast scenario and allows to monitor the evolution of the hemorrhage. Fig. 6 shows the results of differential 3D UWB-MC imaging. To obtain this reconstruction, we have supposed to have reference data obtained when the patient arrives at the emergency unit having a small intracerebral hemorrhage of 5 mm. This reference measurement has been subtracted to a second image presenting a bigger hemorrhage of 10 mm. By doing so, the stroke can be detected and its evolution tracked.

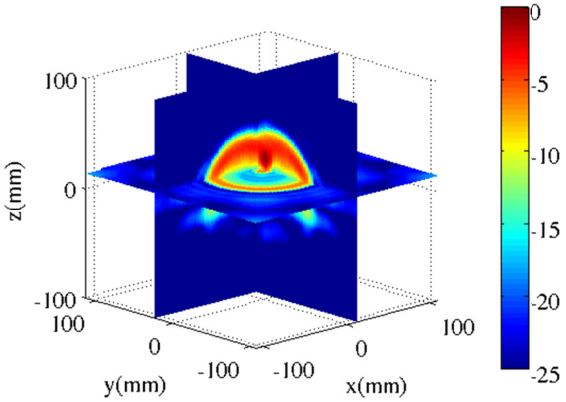

(a)

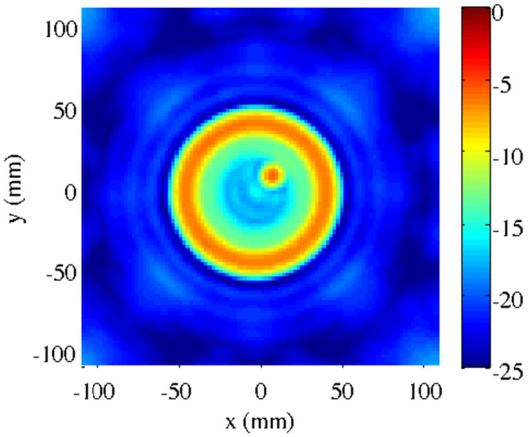

(b)

Fig. 4. 3D UWB-MC reconstructions of the simplified breast model. (a) 3D view. (b) XY cut.

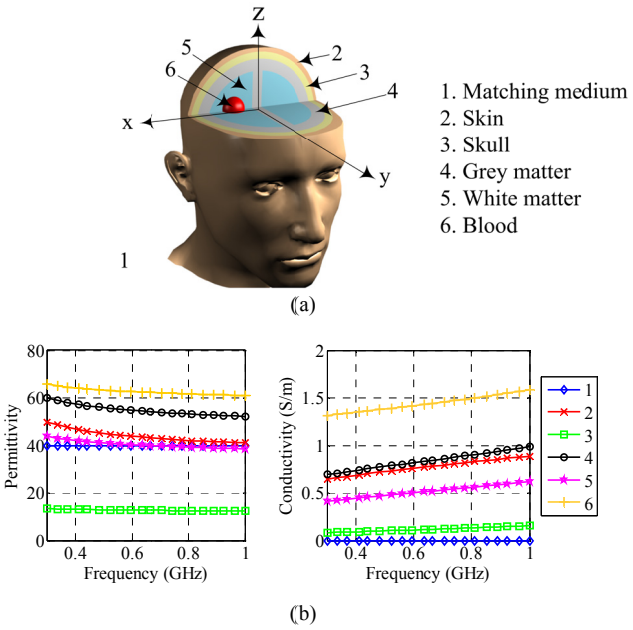

(a) (b)

Fig. 5. (a) Simplified brain model composed by a thin skin layer, the skull, and the two brain hemispheres of white matter covered by a layer of gray matter and a spherical blood hemorrhage. (b) Permittivity and conductivity values of the model.

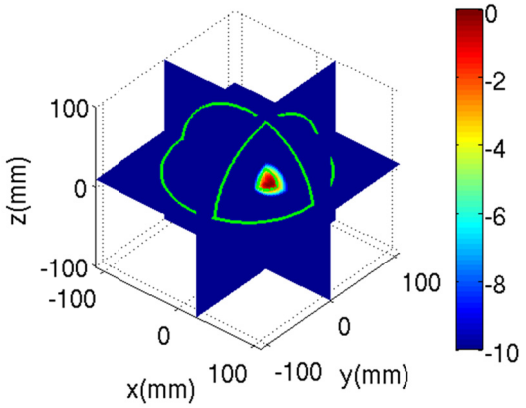

Fig. 6. 3D view of the differential UWB-MC reconstruction of the simplified brain model.

4. Experimental Results

The aim of this section is to assess the potentiality of 3D UWB-MC algorithm deal with experimental measurements, rather than presenting the experimental system itself. The initial measurements have been obtained with the setup shown in Fig. 7. A cylindrical sampling for both transmitting and receiving antennas is accomplished by constructing two virtual arrays moving two antennas by means of a compound positioning system. Revolution symmetry phantoms (around z-axis) will be considered so as to reduce the setup complexity to 3 degrees of freedom provided by 2 linear positioners and a single rotary stage. A linear positioner is used to move the phantom up and down; the rotary stage confers the rotation on one antenna,

while the other antenna moves up and down thanks to the other linear positioner. The remaining measurements can be obtained by taking advantage of the symmetry. A VNA is responsible for the signal generation and reception, and finally the whole procedure can be remotely controlled by a computer. The measured phantom consists of a small clay sphere ($\epsilon'_{clay} = 5.5$) lodged into a paraffin sphere ($\epsilon'_{par} = 2.19$) fixed with a PVC rod ($\epsilon'_{PVC} = 2.9$) from the top, as depicted in Fig. 7. At the current stage of development, the 3D cylindrical measurement system does not permit to use any liquid as matching media, and hence the phantom will be surrounded by air.

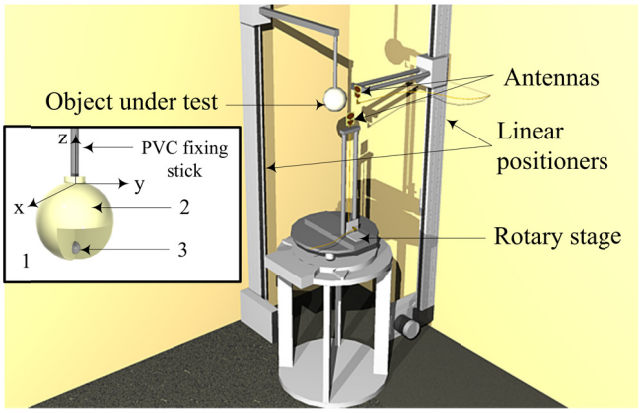

Fig. 7. Experimental setup with 3 degrees of freedom permitting a quasi-cylindrical scan of the target. The target consists of a clay sphere inside a paraffin sphere supported by a PVC rod.

Preliminary reconstructions of simple objects inside water using the 2D version of UWB-MC algorithm have been presented in [16]. Working in air as external medium the phantom constituents have been chosen considering its permittivity to reproduce contrast ratios similar to the biomedical simulated ones, while avoiding large contrasts compared to the air. Moreover, to obtain comparable reconstructions in terms of spatial resolution between measurements and simulations (where a matching medium of high permittivity has been employed) a frequency range between 3 – 10 GHz has been used in the measurements.

Figs. 8(a) and 8(b) present the imaging results from the measured data. Fig. 8(a) shows the reconstruction of external appearance of the phantom composed by superimposing horizontal planes at different heights. The contour of the paraffin sphere and the PVC fixing road are well reconstructed, and even the transition between both structures is represented with good accuracy. Fig. 8(b) shows the correct detection of the internal sphere.

5. Conclusions

In this paper, the potentiality of 3D UWB Magnitude-Combined tomographic algorithm has been assessed for two well-known biomedical applications. The 3D extension and the so-called UWB Magnitude-Combined technique constitute the two main contributions of this algorithm. The

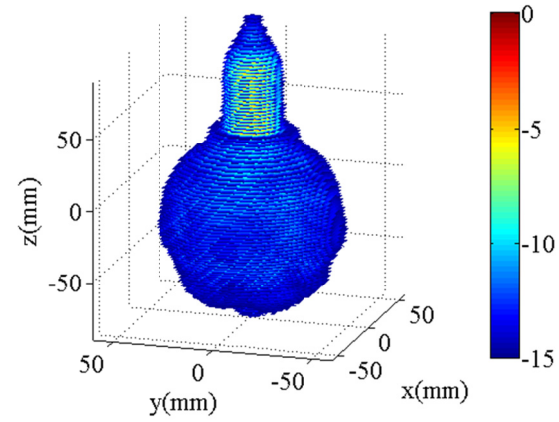

(a)

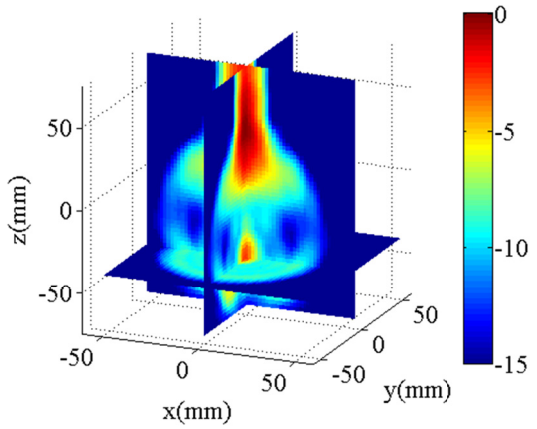

(b)

Fig. 8. (a) External appearance of the 3D UWB-MC reconstruction of the experimental measurement of the two nested spheres. (b) Internal 3D view.

proposed multi-frequency combination contributes to enhance the robustness of the final image to frequency selective artifacts and relatively large and contrasted targets.

For the validation, simplified breast and brain models have been reconstructed, taking into account the frequency dispersive permittivities and conductivities of the tissues. UWB-MC algorithm has reported satisfactory reconstructions for the breast cancer detection application in a particular case where the contrast between the breast tissue and the tumor is low. While this is a challenging case for radar-based algorithms [17], it is more favorable for linearized tomography. On the other hand, brain stroke detection constitutes a more challenging application due to the successive lossy and highly-contrasted layers. To this extent, a differential treatment has to be used, allowing to monitor the evolution of a intracerebral hemorrhage.

Finally a cylindrical measurement system with 3 degrees of freedom has been constructed, and first images of experimental data have been obtained for canonical phantoms, showing robust reconstructions and encouraging results.

Acknowledgements

This work was supported in part by Spanish Interministerial Commission on Science and Technology (CICYT) under projects TEC2007-66698-C04-01, TEC2010-20841-C04-02 and CONSOLIDER CSD2008-68 and by the Ministerio de Educación y Ciencia through the FPU fellowship program.

References

[1] NASS, S. J., HENDERSON, I. C., LASHOF, J. C. *Mammography and Beyond: Developing Technologies for the Early Detection of Breast Cancer*. Washington D.C. (USA), National Academies Press, 2001.

[2] LAZEBNIK, M., McCARTNEY, L., POPOVIC, D., WATKINS, C. B., LINDSTROM, M. J., HARTER, J., SEWALL, S., MAGLIOCCO, A., BOOSKE, J. H., OKONIEWSKI, M., HAGNESS, S. C. A large-scale study of the ultrawideband microwave dielectric properties of normal, benign and malignant breast tissues obtained from cancer surgeries. *Physics in Medicine and Biology*, 2007, vol. 52, no. 20, p. 6093 - 5115.

[3] XU, L., BOND, E. J., VAN BEEN, B. D., HAGNESS, S. C. An overview of ultra-wideband microwave imaging via space-time beamforming for early-stage breast-cancer detection. *IEEE Antennas and Propagation Magazine*, 2005, vol. 47, no. 1, pp. 19 - 34.

[4] FHAGER, A., PERSSON, M. Using a priori data to improve the reconstruction of small objects in microwave tomography. *IEEE Transactions on Microwave Theory and Techniques,* 2007*,* vol. 55, no. 11, p. 2454 - 2462.

[5] GILMORE, C., ABUBAKAR, A., HU, W, HABASHY, T. M., VAN DEN BERG, P. M. Microwave Biomedical Data Inversion Using the Finite-Difference Contrast Source Inversion Method. *IEEE Transactions on Antennas and Propagation,* 2009, vol. 57, no. 5, p. 1528 - 1538.

[6] De ZAEYTIJD, J., FRANCHOIS, A., EYRAUD, C., GREFFIN, J. M. Full-wave three-dimensional microwave imaging with a regularized Gauss-Newton method theory and experiment. *IEEE Transactions on Antennas and Propagation*, 2007, vol. 55, no. 11, p. 3279 - 3292.

[7] SEMENOV, S., BULYSHEV, A., SOUVOROV, A., NAZAROV, A., SIZOV, Y., SVENSON, R., POSUKH, A., PAVLOVSKY, A., REPIN, P., TATSIS, G. Three-dimensional microwave tomography: experimental imaging of phantoms and biological objects. *IEEE Transactions on Microwave Theory and Techniques*, 2000, vol. 48, no. 6, p. 1071 - 1074.

[8] GOLNABI, A. H., MEANEY, P. M., GEIMER, S., PAULSEN, K. D. Microwave imaging for breast cancer detection and therapy monitoring. In *IEEE Topical Conference on Biomedical Wireless Technologies, Networks, and Sensing Systems (BioWireleSS).* Phoenix (AZ, USA), 2011*,* 59 - 62.

[9] RIUS, J. M., PICHOT, C., JOFRE, L., BOLOMEY, J. C., JOACHIMOWICZ, N., BROQUETAS, A., FERRANDO, M. Planar and cylindrical active microwave temperature imaging: numerical simulations. *IEEE Transactions on Medical Imaging,* 1992*,* vol. 11, no. 4, p. 457 - 469.

[10] JOFRE, L., HAWLEY, M. S., BROQUETAS, A., DE LOS REYES, E., FERRANDO, M., ELIAS-FUSTE, A. R. Medical imaging with a microwave tomographic scanner. *IEEE Transactions on Biomedical Engineering,* 1990, vol. 37, no. 3, p. 303 - 312.

[11] JOFRE, L., BROQUETAS, A., ROMEU, J., BLANCH, S., PAPIÓ, A., FABREGAS, X., CARDAMA, A. UWB tomographic radar imaging of penetrable and impenetrable objects. *Proceedings of the IEEE*, 2009, vol. 97, no. 2, p.451 - 464.

[12] GUARDIOLA, M., CAPDEVILA, S., JOFRE, L. UWB-bi-focusing tomography for breast tumor detection. In *Proceedings of the 3rd European Conference on Antennas and Propagation EuCAP 2009*. Berlin (Germany), 2009, p. 1855 - 1859.

[13] SEMENOV, S. Y., CORFIELD, D. R. Microwave tomography for brain imaging: Feasibility assessment for stroke detection. *International Journal of Antennas and Propagation*, 2008, vol. 2008, 8 pages.

[14] SLANLEY, M., KAK, A., LARSEN, L. Limitations of imaging with first order diffraction tomography. *IEEE Transactions on Microwave Theory and Techniques*, 1984, vol. 32, no. 8, p. 860 - 874.

[15] ROMEU, J., JOFRE, L. Truncation errors in cylindrical near to far field transform. A plane wave synthesis approach. In *Proceedings of the 22nd European Microwave Conference*, 1992, vol. 1, p. 659 - 663.

[16] GUARDIOLA, M., FHAGER, A., JOFRE, L., PERSSON, M. Circular microwave tomographic imaging. Experimental comparison between quantitative and qualitative algorithms. In *Proceedings of the 5th European Conference on Antennas and Propagation EuCAP 2011*. Rome (Italy), 2011.

[17] KLEMM, M., CRADDOCK, I. J., LEENDERTZ, J. A., PREECE, A., BENJAMIN, R. Radar-based breast cancer detection using hemispherical antenna array – Experimental results. *IEEE Transactions on Antennas and Propagation*, 2009, vol. 57, no. 6, p. 1692 - 1704.

About Authors ...

Marta GUARDIOLA was born in Besalú, Spain, in 1984. She received the Telecommunication Engineer degree and the European Master of Research on Information and Communication Technologies (MERIT) from the Technical University of Catalonia (UPC) in 2008 and 2009 respectively. Since September 2009 she is pursuing her PhD degree at the Communications Department of the Telecommunication Engineering School at the UPC. Her research interests include microwave imaging algorithms and systems for biomedical applications and UWB antennas.

Lluís JOFRE was born in Canet de Mar, Spain, in 1956. He received the M.Sc. (Ing) and Ph.D. (Doctor Ing.) degrees in electrical engineering (telecommunication engineering), from the Technical University of Catalonia (UPC), Barcelona, Spain, in 1978 and 1982, respectively. From 1979 to 1980, he was a Research Assistant with the Electrophysics Group, UPC, where he worked on the analysis and near field measurement of antennas and scatterers. From 1981 to 1982, he was with the École Supérieure d'Electricité, Paris, France, where he was involved in microwave antenna design and imaging techniques for medical and industrial applications. Since 1982, he has been with the Communications Department, Telecomunication Engineering School, UPC, as an ssociate Professor first and, then, as a Full Professor since 1989. From 1986 to 1987, he was a Visiting Fulbright Scholar at

the Georgia Institute of Technology, Atlanta, where he worked on antennas and electromagnetic imaging and visualization. From 1989 to 1994, he was the Director of the Telecommunication Engineering School, UPC, and from 1994 to 2000, he was the UPC Vice-Rector for Academic Planning. From 2000 to 2001, he was a Visiting Professor at the Electrical and Computer Engineering Department, Henry Samueli School of Engineering, University of California, Irvine. From 2002 to 2004, he was the Director of the Catalan Research Foundation, and since 2003, he has been the Director of the UPC-Telefónica Chair and director of the Promoting Engineering Catalan Program EnginyCAT. He is a member of different Higher Education Evaluation Agencies at Spanish and European level. From December 2011, he is the General Director of Universities in the Economy and Knowledge Council of the Catalan Government. At international level, he is a Fellow of the IEEE Society. He has published more than 100 scientific and technical papers, reports, and chapters in specialized volumes. His research interests include antennas, electromagnetic scattering and imaging, and system miniaturization for wireless and sensing industrial and bio-applications. He has published more than 100 scientific and technical papers, reports and chapters in specialized volumes.

Santiago CAPDEVILA was born in Barcelona, Spain, in 1982. He received the M.Sc. (Ing) degree in Electrical Engineering (Telecommunications eng.) from the Technical University of Catalonia (UPC) in 2006. He is currently a PhD. Candidate at the AntennaLab Group, Signal Theory and Communications Department, UPC. His research interests include nano-antennas, radio frequency identification, imaging and sensors.

Sebastián BLANCH was born in Barcelona, Spain, in 1961. He received the Ingeniero and Doctor Ingeniero degrees in Telecommunication Engineering, both from the Polytechnic University of Catalonia (UPC), Barcelona, Spain, in 1989 and 1996, respectively. In 1989, he joined the Electromagnetic and Photonics Engineering Group of the Signal Theory and Communications Department. Currently, he is Associate Professor at UPC. His research interests are antenna near field measurements, antenna diagnostics, and antenna design.

Jordi ROMEU was born in Barcelona, Spain in 1962. He received the Ingeniero de telecomunicación and Doctor Ingeniero de Telecomunicación, both from the Universitat Politècnica de Catalunya (UPC) in 1986 and 1991, respectively. In 1985, he joined the Photonic and Electromagnetic Engineering group, Signal theory and Communications Department, UPC. Currently he is Full Professor there, where he is engaged in research in antenna near-field measurements, antenna diagnostics, and antenna design. He was visiting scholar at the Antenna Laboratory, University of California, Los Angeles, in 1999, on a NATO Scientific Program Scholarship, and in 2004 at University of California Irvine. He holds several patents and has published 35 refereed papers in international jounals and 50 conference proceedings. Dr. Romeu was grand winner of the European IT Prize, awarded by the European Commission, for his contributions in the development of fractal antennas in 1998.